Stem Cell Reports, Volume *16*

Supplemental Information

Sonlicromanol improves neuronal network dysfunction and transcriptome changes linked to m.3243A>G heteroplasmy in iPSC-derived neurons

Teun M. Klein Gunnewiek, Anouk H.A. Verboven, Iris Pelgrim, Mark Hogeweg, Chantal Schoenmaker, Herma Renkema, Julien Beyrath, Jan Smeitink, Bert B.A. de Vries, Peter-Bram A.C. 't Hoen, Tamas Kozicz, and Nael Nadif Kasri

Supplemental information

Supplemental information includes the six supplemental figures, three supplemental tables, and supplemental experimental procedures.

Supplemental items

Figure S1. Density images, LH3 developmental timeline from DIV16-44, and MEA data from the DIV30-44 developmental timeline, for lines LH1-3 and HH1-3, Related to Figure 1.
Figure S2. Principal component analysis on RNA-seq samples from iNeurons co-cultured with astrocytes, Related to Figure 3, 4 and 6.
Figure S3. MEA data for sonlicromanol (KH176) treatment at mature network age (DIV29), Related to Figure 5.
Figure S4. Propidium iodide staining to quantify cell death; neuronal density quantified by MAP2 positive cells; m.3243A>G heteroplasmy levels, Related to Figure 5.
Figure S5. DNA damage due to oxidative stress levels in the neuronal soma, Related to Figure 5.
Figure S6. Gene expression changes in HH vs LH iNeurons for isogenic set 2, Related to Figure 6.

Supplemental tables (added as separate excel files)

Table S1: Results from differential expression analysis and gene set enrichment analysis for HH1+HH2 vs LH1+LH2 neurons, Related to Figure 3. Differential expression analysis results for genes of interest for HH1+HH2 vs LH1+LH2, Related to Figure 3. Results from differential expression analysis and gene set enrichment analysis for astrocytes co-cultured with HH1+HH2 vs astrocytes co-cultured with LH1+LH2 neurons, Related to Figure 4.

Table S2: Results from differential expression analysis and gene set enrichment analysis for HH1 vs LH1 neurons, Related to Figure 6. Results from differential expression analysis and gene set enrichment analysis for HH1+KH176 vs HH1 neurons, Related to Figure 6.

Table S3: Results from differential expression analysis and gene set enrichment analysis for HH2 vs LH2 neurons, Related to Figure S6. Results from differential expression analysis and gene set enrichment analysis for HH2+KH176 vs HH2 neurons, Related to Figure S6.

Supplemental Experimental Procedures

RNA-seq library preparation
RNA-seq data analysis
RNA-seq data visualization
8-OXO-dg fluorescence
Propidium Iodide

Supplemental items

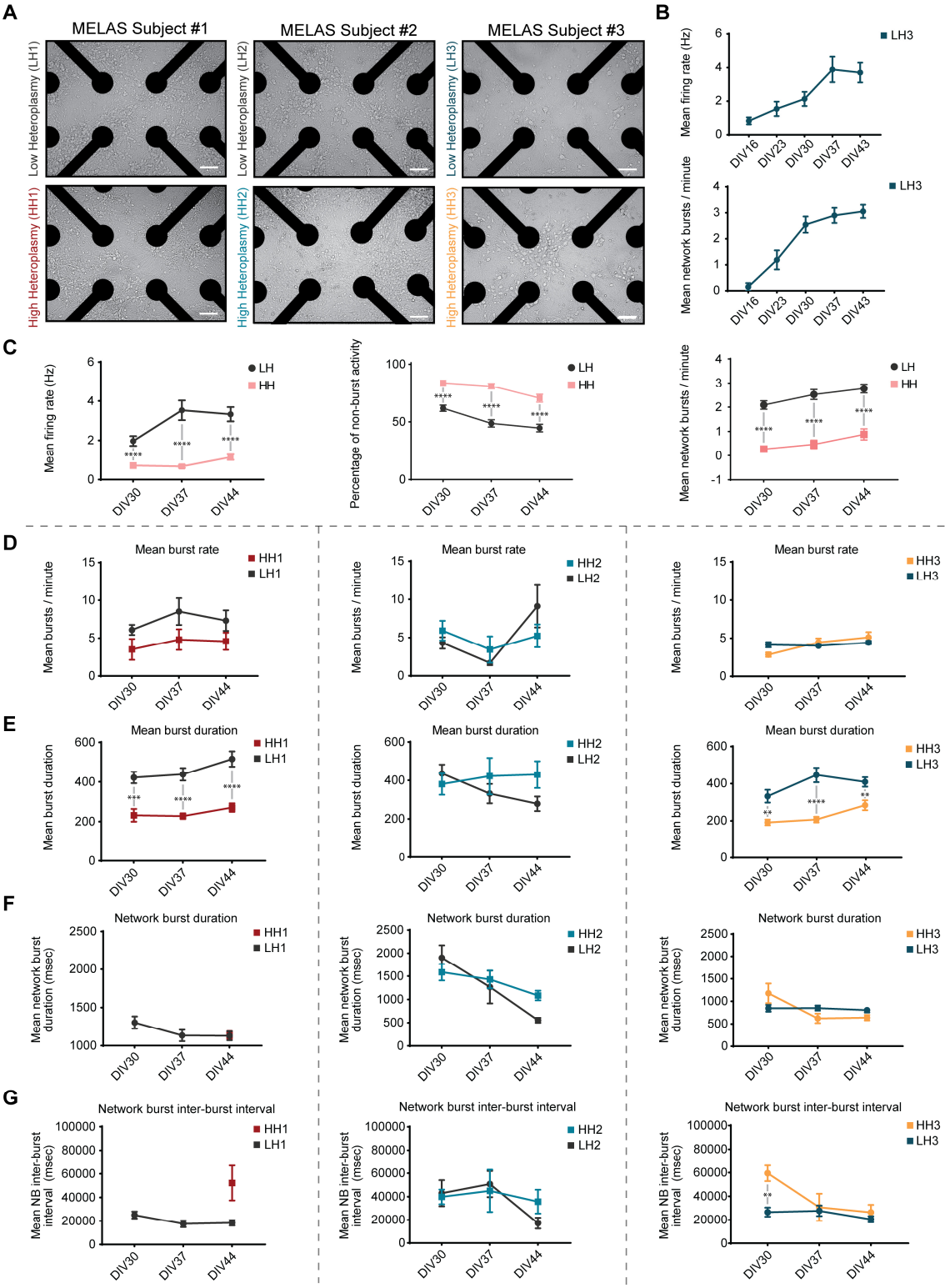

Figure S1. Density images, LH3 developmental timeline from DIV16-44, and MEA data from the DIV30-44 developmental timeline, for lines LH1-3 and HH1-3, Related to Figure 1. (A) Light fluorescence image showing density images for LH1-3 and HH1-3 (scale bar = 100 μm). (B) LH3 MEA

networks were recorded from DIV16-44 and were quantified based on the mean number of spikes per minute (mean firing rate; Hz) and mean number of synchronous network bursts per minute (network burst rate). LH1-3 and HH1-3 MEA networks were recorded from DIV30-44 and (C) pooled and quantified based on the mean firing rate (Hz), the mean percentage of non-burst activity, and the mean network burst rate (per minute). LH1-3 and HH1-3 MEA networks were separately quantified based on (D) the mean number of bursts per minute (Mean burst rate), (E) the mean burst duration (msec), (F) the mean network burst duration, and (G) the mean inter-network burst interval (msec) for LH1 (n=27) and HH1 (n=27), LH2 (n=16) and HH2 (n=14), and LH3 (n=23) and HH3 (n=21). Data represent means ± SEM. *p<0.05, **p<0.01, ***p<0.001, ****p<0.0001, using restricted maximum likelihood model, with Holm-Sidak's correction for multiple comparisons between treated and untreated samples. We could not calculate statistical significance for the network-inter burst interval for isogenic set 1 due to the low number of replicates that show a network burst number of 3 or more.

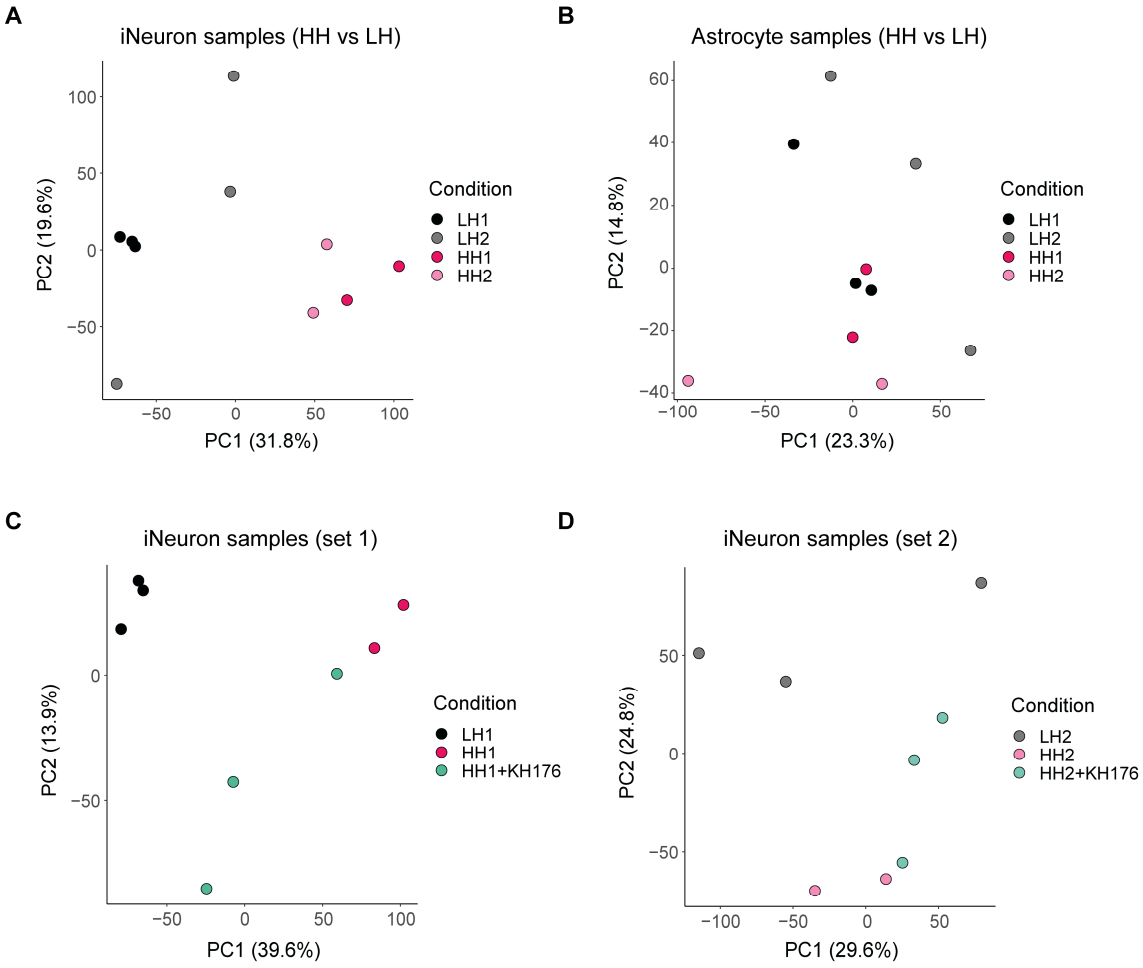

Figure S2. Principal component analysis on RNA-seq samples from iNeurons co-cultured with astrocytes, Related to Figure 3, 4 and 6. (A) Principal component analysis (PCA) plots displaying PC1 and PC2 for (A) LH (n=6) and HH (n=4) iNeurons, (B) astrocytes co-cultured with LH (n=6) or HH (n=4), (C) LH1 (n=3), HH1 (n=2) and HH1+KH176 (n=3) iNeurons, and (D) LH2 (n=3), HH2 (n=2) and HH2+KH176 (n=3) iNeurons. In all cases, iNeurons were co-cultured with rat astrocytes. For iNeuron gene expression profiles, reads uniquely mapping to the human genome were extracted. For astrocyte gene expression profiles, reads uniquely mapping to the rat genome were extracted.

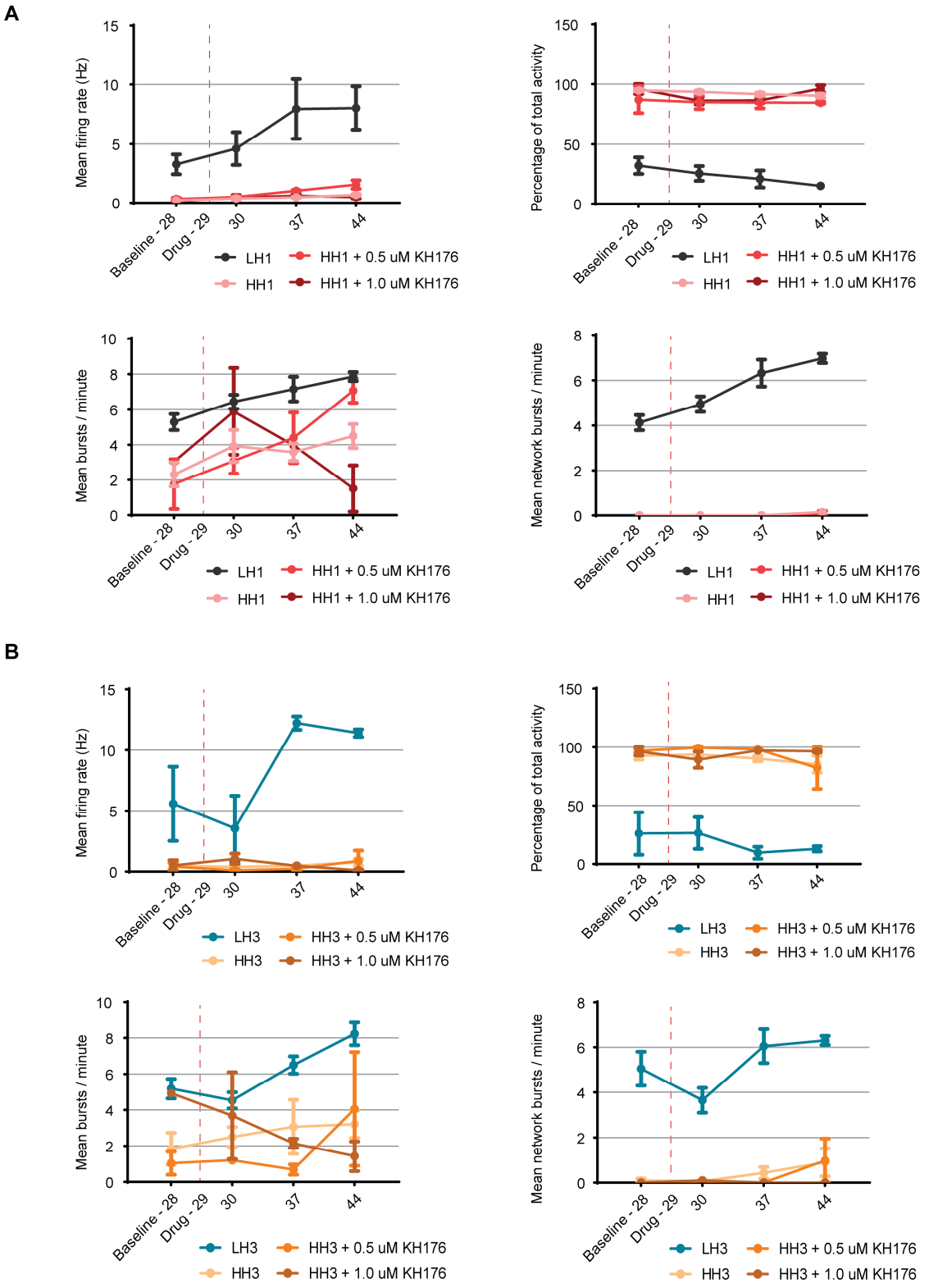

Figure S3. MEA data for sonlicromanol (KH176) treatment at mature network age (DIV29), Related to Figure 5. HH1 and HH3 cultures were treated from DIV29 onwards with either 0.5 µM or 1.0 µM KH176 and recorded for 10 minutes of neuronal network activity on MEA for LH1 (n=6), HH1 (n=12), HH1 + 0.5 µM KH176 (n=4), HH1 + 1 µM KH176 (n=4), LH3 (n=6), HH3 (n=6), HH3 + 0.5 µM KH176 (n=4), HH3 + 1 µM KH176 (n=4). We quantified the mean firing rate (Hz), the mean percentage

of random activity (%), the mean number of bursts per minute (burst rate), and the mean number of network bursts per minute for (A) isogenic set 1 and (B) isogenic set 3 and determined the statistical difference between the untreated- and sonlicromanol treated HH1-3 conditions. None of the sonlicromanol-treated HH1-3 conditions were significantly different from untreated HH1-3 conditions. Data represent means ± SEM. Tested using restricted maximum likelihood model, with Holm-Sidak's correction for multiple comparisons between treated and untreated samples.

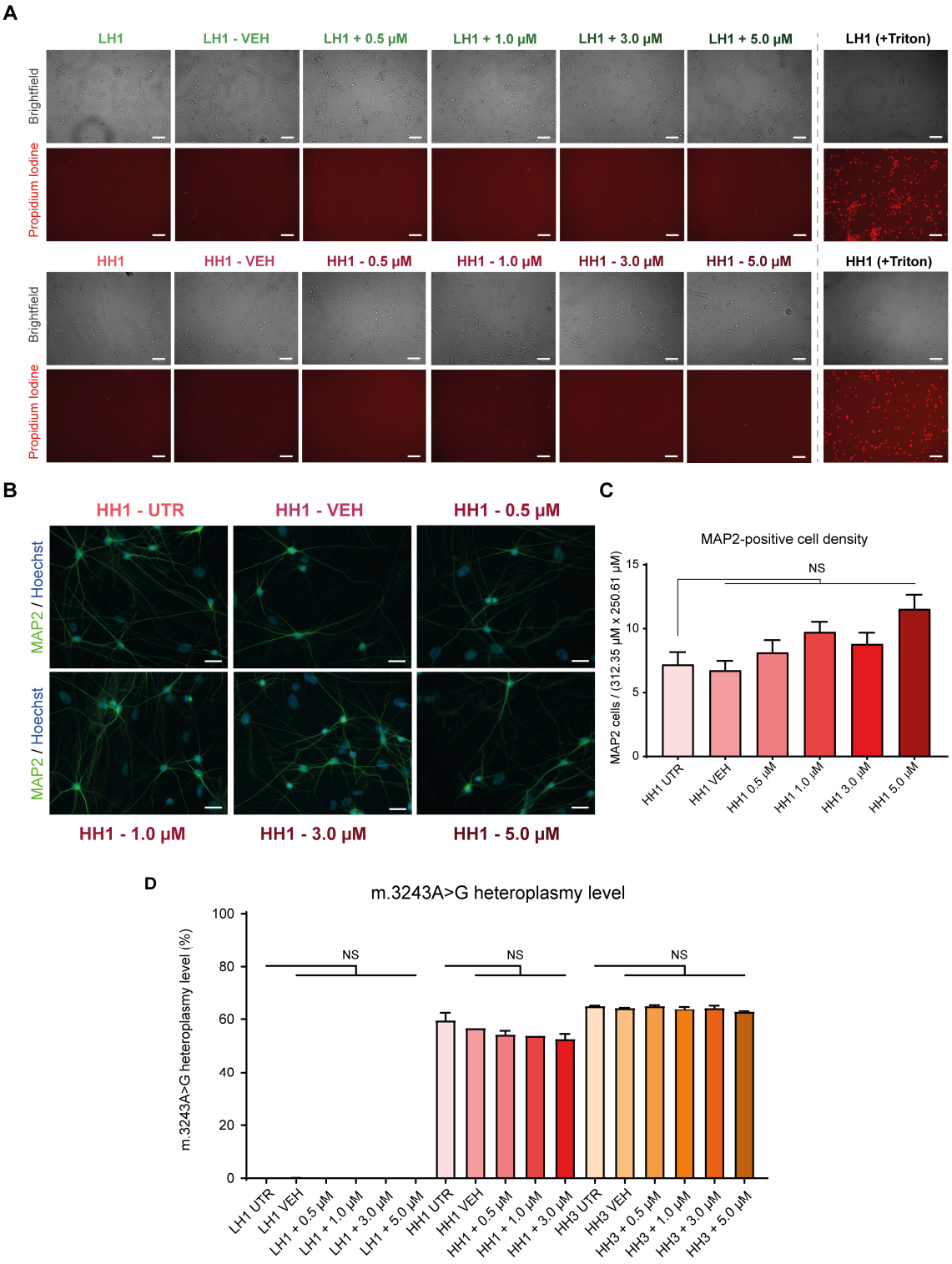

Figure S4. Propidium iodide staining to quantify cell death; neuronal density quantified by MAP2 positive cells; m.3243A>G heteroplasmy levels, Related to Figure 5. (A) Brightfield images showing the comparable densities between untreated- and sonlicromanol treated LH1 and HH1 neurons at DIV44 (scale bar = 100 µm). The fluorescent propidium iodide stainings (bottom rows) revealed little to no cell death in the experimental conditions. LH1 and HH1 samples were treated for 15 minutes with 0.2% Triton-X, serving as positive controls for propidium iodide signal, and showing clear red fluorescent cells. (B) Cell density was further quantified using MAP2 staining at DIV44 (scale bar = 30

μm). (C) No differences were observed in the number of MAP2 positive cells between untreated- and KH176 treated HH1 cultures, indicating no substantial effect of sonlicromanol on neuronal survival and eventual culture density. MAP2 positive cell density was calculated by counting MAP2 positive cells on 15 random images, at 40X, and averaging density over the 312.35 μM x 250.61 μM surface area. Data represent means ± SEM. *p<0.05, **p<0.01, ***p<0.001, ****p<0.0001, using one-way ANOVA using Bonferroni correction for multiple testing. (D) m.3243A>G heteroplasmy levels were quantified for untreated- and sonlicromanol treated LH1, HH1, and HH3 neuronal cultures at DIV44 (n=2-4), which showed no differences. Data represent means ± SEM. *p<0.05, **p<0.01, ***p<0.001, ****p<0.0001, using one-way ANOVA using Bonferroni correction for multiple testing.

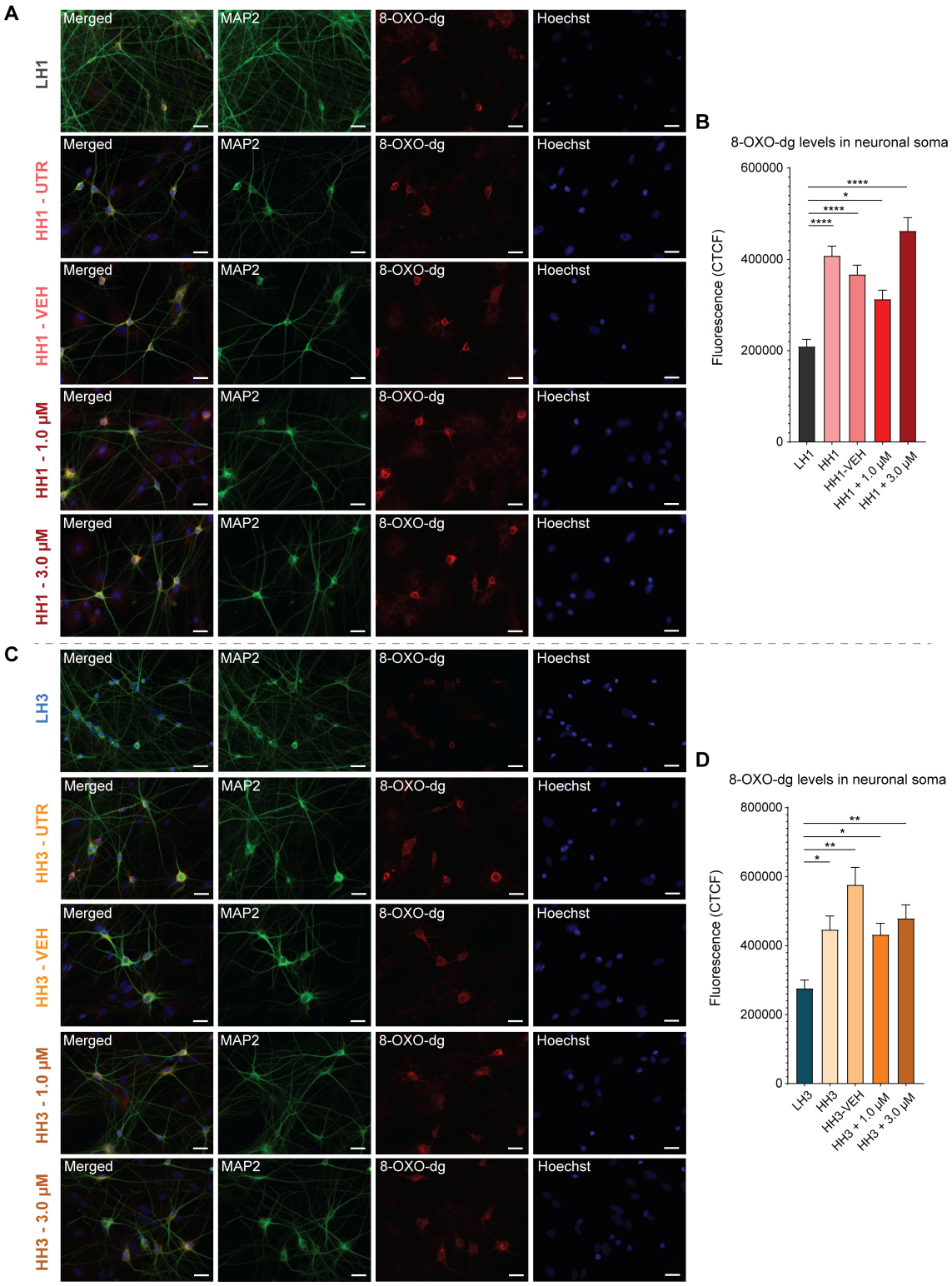

Figure S5. DNA damage due to oxidative stress levels in the neuronal soma, Related to Figure 5. (A) Neurons at DIV30 were stained for 8-OXO-dg, a measure of local oxidative stress, after which relative fluorescence in the neuronal soma was measured and compared between untreated- and treated HH1 and HH3 (scale bar = 30 µm). (B) Bar plot showing the 8-OXO-dg corrected total cell fluorescence (CTCF) comparison for LH1 (n=27), HH1 (n=27), HH1-veh (n=29), HH1 + 1.0 µM KH176 (n=24), and HH1 + 3.0 µM KH176 (n=34). Data represent means ± SEM. *p<0.05, **p<0.01, ***p<0.001,

****p<0.0001, using one-way ANOVA using Bonferroni correction for multiple testing. (C) Neurons were stained for 8-OXO-dg, a measure of local oxidative stress, after which relative fluorescence in the neuronal soma was measured (scale bar = 30 μm). (D) Bar plot showing the 8-OXO-dg corrected total cell fluorescence (CTCF) comparison for LH3 (n=19), HH3 (n=31), HH3-veh (n=29), HH3 + 1.0 μM KH176 (n=27), and HH3 + 3.0 μM KH176 (n=40). Data represent means ± SEM. *p<0.05, **p<0.01, ***p<0.001, ****p<0.0001, using one-way ANOVA using Bonferroni correction for multiple testing.

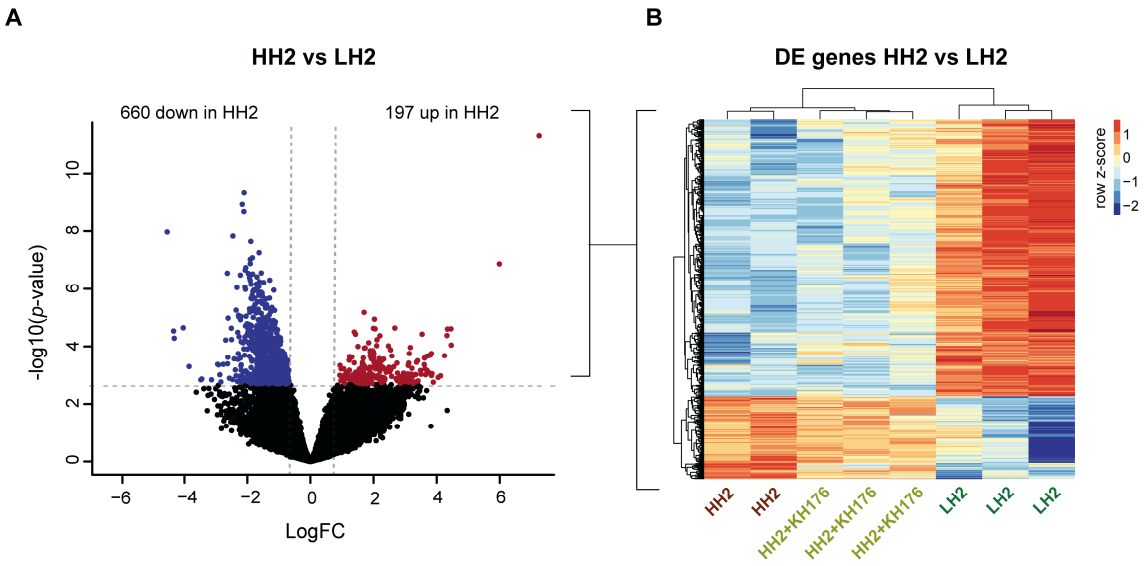

Figure S6. Gene expression changes in HH vs LH iNeurons for isogenic set 2, Related to Figure 6. (A) Volcano plot showing DE genes in HH2 versus LH2 iNeurons (genes with adj. p<0.05 are labelled), with up-regulated genes in red (logFC>0) and down-regulated genes in blue (logFC<0). (B) Heatmap showing expression of DE genes in HH2 vs LH2, for LH2 (n=3), HH2 (n=2) and HH2+KH176 (n=3) samples. Voom-transformed and batch-corrected counts per million (log2 scale) were scaled per gene.

Supplemental Experimental Procedures

RNA-seq library preparation

For each sample, 25 ng total RNA (in 0.65 µL) was mixed with 0.1 µL dNTP mix (10 mM each) (Invitrogen, 10297018), 0.3 µL nuclease-free water (NF H2O) and 0.4 µL anchored oligo-dT (2.5 µM) primer(5'-ACGACGCTCTTCCGATCTNNNNNNNN[10bpindex]TTTTTTTTTTTTTTTTTTTTTTTTTTTTTTVN-3', where "N" is any base and "V" is either "A", "C" or "G"; IDT) in a tube containing 7 µL Vapor-Lock (Qiagen, 981611). Each sample was incubated for 5 min at 65°C and directly placed on ice. First strand reaction mix was added, consisting of 0.4 µL Maxima RT buffer (5X) (Thermo Scientific, EP0751), 0.05 µL RNasin Plus (Promega, N2611) and 0.1 µL Maxima H Minus Reverse Transcriptase (Thermo Scientific, EP0751). Reverse transcription was performed by incubation at 50°C for 30 min and terminated by heating at 85°C for 5 min. 2 µL RT product was mixed with 7.7 µL NF H2O, 2.5 µL Second Strand Buffer (Invitrogen, 10812014), 0.25 µL dNTP mix (10 mM each), 0.35 µL DNA polymerase I (E. coli) (NEB, M0209), 0.09 µL DNA ligase (E. coli) (NEB, M0205) and 0.09 µL Ambion RNase H (E. coli) (Invitrogen, AM2293). Second strand synthesis was performed by incubation at 16°C for 150 min, followed by 75°C for 20 min. 0.5 µL Exonuclease I (NEB, M0293) was added per sample and incubated at 37°C for 60 min. cDNA samples were pooled per sets of 8, randomized across three pools. Vapor-Lock was removed, and samples were added up with NF H2O to a total volume of 107.6 µL. Each pool of samples was purified using 79 µL beads buffer (20% PEG-8000 in 2.5 M NaCL, final concentrations) and 50 µL Ampure XP Beads (Beckman Coulter, A63881), and eluted in 7 µL NF H2O.

Tagmentation was performed per pool by adding 5.5 µL double-stranded cDNA sample to 5.0 µL Nextera TD buffer (Illumina, 15027866), and 1.5 µL TDE1 Enzyme (Illumina, 15027865), incubated at 55°C for 5 min. Samples were directly placed on ice for at least 3 min. The reaction was terminated by adding 12 µL Buffer PB (QiaQuick, 19066) and incubating for 5 min at room temperature. Samples were purified using 48 µL Ampure XP beads and eluted in 10 µL NF H2O. Next, each sample was mixed with 2 µL P5 primer (10 µM), (5'-AATGATACGGCGACCACCGAGATCTACAC[i5]ACACTCTTTCCCTACACGACGCTCTTCCGATCT-3'; IDT), 2 µL P7 primer (10 µM) (5'-CAAGCAGAAGACGGCATACGAGAT[i7]GTCTCGTGGGCTCGG-3'; IDT), 6 µL NF H2O, and 20 µL NEBNext High-Fidelity 2X PCR Master Mix (NEB, M0541). Amplification was performed using the following program: 72°C for 5 min, 98°C for 30 sec, 15 cycles of (98°C for 10 sec, 66°C for 30 sec, 72°C for 1 min) and a final step at 72°C for 5 min. Samples were purified using 32 µL Ampure XP beads and eluted in 14 µL NF H2O. Libraries were visualized by electrophoresis on a 1% agarose and 1X TAE gel containing 0.3 µg/mL ethidium bromide (Invitrogen, 15585011). Gel extraction was performed to select products between 200 – 1000 bp using the Nucleospin Gel and PCR Clean-up kit (Macherey-Nagel, 740609). Samples were eluted in 15 µL NF H2O. cDNA concentrations were measured by Qubit dsDNA HS Assay kit (Invitrogen, Q32854). Product size distributions were visualized using Agilent's Tapestation system (D5000 ScreenTape and Reagents, 5067-5588/9). Libraries were sequenced on the NextSeq 500 platform (Illumina) using a V2 75 cycle kit (Read 1: 18 cycles, Read 2: 52 cycles, Index 1: 10 cycles).

RNA-seq data analysis

For differential expression analysis with limma, a linear regression model was fit, in which the voom-transformed expression values were modelled as a function of the condition (LH untreated, HH untreated, HH treated), the isogenic set (set#1, set#2), and MEA batch (plate 1, plate 2). For DE analysis between HH and LH lines, a contrast was defined comparing HH untreated with LH untreated samples using the following design formula: model.matrix(~0+condition+set+MEA). DE analysis on RNA-seq data from astrocytes co-cultured with HH and LH iNeurons was performed using the same approach. For DE analysis between HH treated and HH untreated samples, pairwise comparisons were made within each isogenic set, using the following design formula: model.matrix(~0+condition+MEA). For the gene set enrichment analysis using fgsea, gene sets were loaded for the correct species (Homo Sapiens or Rattus Norvegicus) per enrichment analysis (iNeuron or rat astrocyte samples, respectively). Gene symbols corresponding to transcripts not part of the final gene list were removed from the selected gene sets. Subsequently, gene sets with remaining gene set size >5 and <500 were used for GSEA. Gene symbols (Ensembl version 94) from the final gene list were converted to gene symbols from Ensembl version 97, corresponding to the version of gene symbols used in MSigDB.

RNA-seq data visualization

Principal component analysis (PCA) was performed on the voom-transformed and batch corrected counts using the prcomp function from stats v3.6.1 (R package). Heatmaps were generated using voom-transformed and batch corrected counts scaled per gene (row z-score), with hierarchical clustering performed on rows and columns, using pheatmap v1.0.12 (R package). A Circos plot was generated using the GOCluster function from GOplot v1.0.2 (R package), showing the logFC for the leading edge genes per gene set.

8-OXO-dg fluorescence

iNeurons were stained and imaged as described above. We used fluorescence level of 8-oxo-dG (8-oxo-2'-deoxyguanosine), oxidized derivative of deoxyguanosine, as indicator for the level of DNA damage due to oxidative stress. At DIV30, cells were fixed and imaged after 24 hour o/n incubation. The corrected total cell fluorescence (CTCF) was calculated in the neuronal soma region of interest (ROI) using ImageJ image software.

Propidium Iodide

Cells at DIV30 were treated for 5 minutes with propidium iodide (PI; ThermoFisher Scientific, BMS500PI) or 15 minutes with PI and 0.2% triton X-100 (Sigma-Aldrich, #9002-93-1). The PI + Triton X-100 treated LH and HH cultures serve as positive control.